IEEE Access
Multidisciplinary ⋮ Rapid Review ⋮ Open Access Journal

Received 11 December 2022, accepted 24 December 2022, date of publication 9 January 2023, date of current version 13 January 2023.

Digital Object Identifier 10.1109/ACCESS.2023.3235597

RESEARCH ARTICLE

Continuous Beam Steering Realized by Tunable Ground in a Patch Antenna

ZHISHU QU[1], YIHUA ZHOU[1], (Graduate Student Member, IEEE), SHAKER ALKARAKI[1], (Member, IEEE), JAMES R. KELLY[1], (Member, IEEE), AND YUE GAO[2], (Senior Member, IEEE)

[1]Electronic Engineering and Computer Science Department, Queen Mary University of London, E1 4NS London, U.K.
[2]School of Computer Science, Fudan University, Shanghai 200438, China

Corresponding author: Yihua Zhou (yihua.zhou@qmul.ac.uk)

This work was supported in part by the Grant from The United Kingdom Engineering and Physical Sciences Research Council under Grant EP/V008420/1, and in part by the Chinese Scholarship Council.

ABSTRACT A continuously steerable patch antenna employing liquid metal is presented. The proposed antenna employs a novel tunable ground plane together with parasitic steering to steer the direction of the main beam. The tunable ground plane consists of a permanent region, made from copper, and two tunable regions formed from liquid metal. The liquid metal channels were fabricated using 3D printing technology. By continuously injecting liquid metal into channels, the proposed patch antenna can provide continuous beam steering from $-30°$ to $+30°$ in the elevation plane, while achieving low side lobe level performance combined with low scan loss performance. Such an approach has never been tried before and it is only possible due to the unique properties of liquid metal. To the best of the authors' knowledge, this is the first time that tunable ground plane has been used for a patch antenna to achieve continuous beam steering. The proposed antenna operates at 5.3 GHz. The antenna is fabricated and measured. Measurement results agree well with the simulation results and validate the effectiveness of the proposed beam steering technique. The proposed antenna has a measured gain of 8.1 dBi at 5.3 GHz and wide bandwidth performance. The tunable ground technique proposed in this work will find numerous applications within future wireless communications systems.

INDEX TERMS 3-D printing, beam scanning, continuous beam steering, liquid metal, microstrip patch antenna, pattern reconfiguration, wide scan angle.

I. INTRODUCTION

Beam steerable antennas are widely used in a range of emerging applications, including radar systems and satellite communications. They have the capability of enhancing communication security, improving channel capacity, and adapting to changing channel conditions [1], [2], [3], [4], [5], [6], [7], [8]. A phased array antenna is a popular example of a beam steerable antenna [9], [10], [11], [12]. A phased array antenna can achieve continuous beam steering. However, it requires phase shifters to control the phase, which are expensive and suffer from high energy losses. Reflect-array or transmit-array antennas can achieve continuous beam steering [13], [14], [15], [16], [17]. However, they consist of many unit cells, which increases the complexity of the structure. A patch antenna is an example of a single-element antenna that can be used as the basis for beam steerable antennas, due to its low cost, simple structure, and ease of fabrication [18], [19].

Previous literature has reported patch antennas which steer beams by changing the ground plane [20], [21], [22], [23]. For example, a reconfigurable patch antenna was proposed in [20]. By tuning on the different combinations of switches, it is possible to connect vertical metal walls to the patch antenna. The beam direction is thus altered by varying the eigenmode supported by the patch antenna. However, the antenna proposed in [20] exhibits more than 2 dB scan loss over a scan angle range of $\pm 20°$. The vertical metal walls also increase the profile of antenna. The antenna proposed in [22] has a

The associate editor coordinating the review of this manuscript and approving it for publication was Debabrata K. Karmokar.

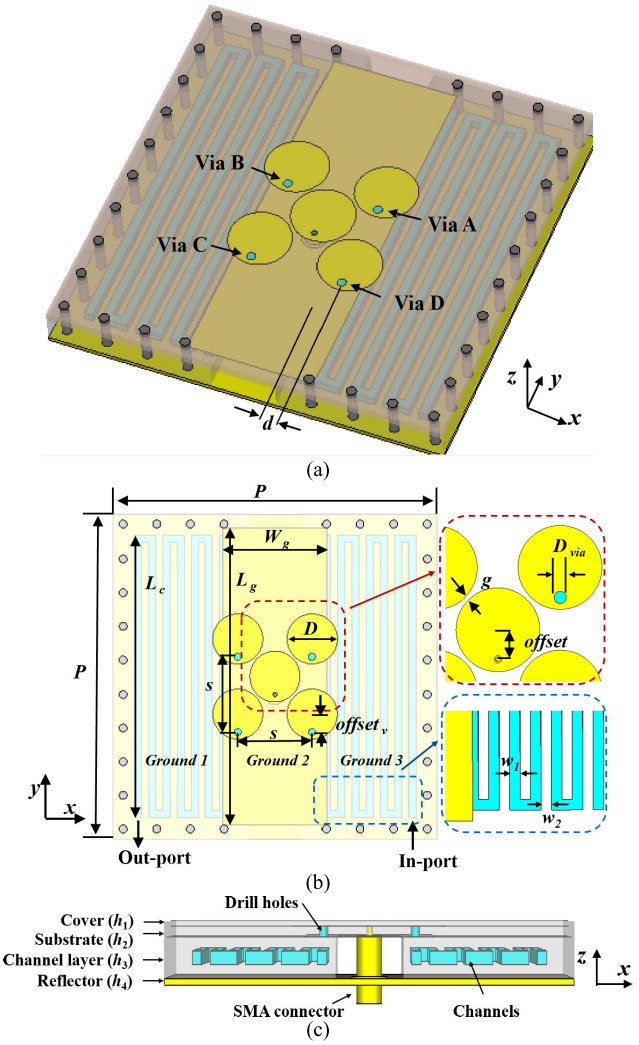

FIGURE 1. Geometry and parameters of the proposed antenna. (a) Perspective view; (b) top view and (c) side view. Key: Yellow parts are copper and blue parts are liquid metal channels.

low profile. It incorporates one slot which acts as a radiator together with four slits which act as parasitics. By tuning on the different switches, located within the slits, it is possible to alter the behavior of the slits and thus achieving the beam reconfiguration. However, the antenna can only steer its beam to a maximum angle of ±15°. More importantly, in the existing literature on patch antennas having a single feed, most designs can only steer beams towards a discrete range of different directions rather than provide continuous beam steering. Only a few papers report that patch antennas with a single feed can achieve continuous beam steering. For example, [24] proposed a beam steerable patch antenna. It used parasitics as directors or reflectors. The movable parasitic director and reflector elements were implemented by liquid metal. The antenna is capable of performing fine resolution beam steering over a 360° range. However, the antenna in [24] has low overall gain performance and it steers the beam in the azimuth plane rather than the elevation plane.

TABLE 1. Dimensions of the proposed antenna (Unit: MM).

P	L_g	L_c	W_g	D	D_{via}	$offset$
91	83	79	29	7	2	4.9
g	w_1	w_2	h_1	h_2	s	$offset_v$
0.7	2	2	0.813	1.524	20.79	4.9
h_3	h_4	d				
6	1	2.9				

We report a patch antenna employing liquid metal that can achieve continuous beam steering in the elevation plane. The proposed antenna has only one single feed. Control of the main beam direction is achieved by continuously tuning sections of ground plane. Such an approach has never been tried before and it is only possible due to the unique properties of liquid metal. Additionally, compared with conventional devices like PIN diodes, liquid metal has the advantages of low insertion loss, low harmonic distortion, large tuning ranges and high-power handling capability. Our design also involves parasitic steering technique, that part of antenna is similar to that described in [25]. However, the design presented in [25] only applies parasitic patches which enabled by PIN diodes, whilst our design combines two different beam steering techniques including: 1) parasitic patches enabled by liquid metal vias and 2) tunable ground plane using liquid metal. This enables our proposed design to have wider bandwidth performance and more importantly able to continuously steer the beam of the antenna up to ±30° with 1.4 dB of scan loss. In addition, the proposed antenna has the potential for improved and higher power handle capability. However, the design in [25] can only discretely switch beam in few steps to a maximum angle of ±15° with 1.3 dB of scan loss. As a result, our design differs from the designs, discussed above, in both approach and performance. The proposed antenna is fabricated and measured at 5.3 GHz. The proposed patch antenna having the capability of continuous beam steering over a wide scan angle range is an attractive candidate for modern wireless communications.

II. ANTENNA DESIGN, OPERATING PRINCIPLE, AND SIMULATION RESULTS

A. ANTENNA DESIGN

Fig. 1 shows the geometry and parameters of the proposed antenna. Table 1 shows the dimensions of the proposed antenna. The antenna is constructed using four layers in total, namely h_1 to h_4. The first layer works as a cover and it is formed from a piece of Rogers RO4003c having a thickness of 0.813 mm, a permittivity of 3.55, and a loss tangent of 0.0027. The second layer works as the substrate of the patch antenna, and it is formed from a piece of Rogers RO4003c having a thickness of 1.524 mm. On the upper surface of the substrate layer, there is a driven patch in the center of the structure surrounded by four parasitics. The driven central

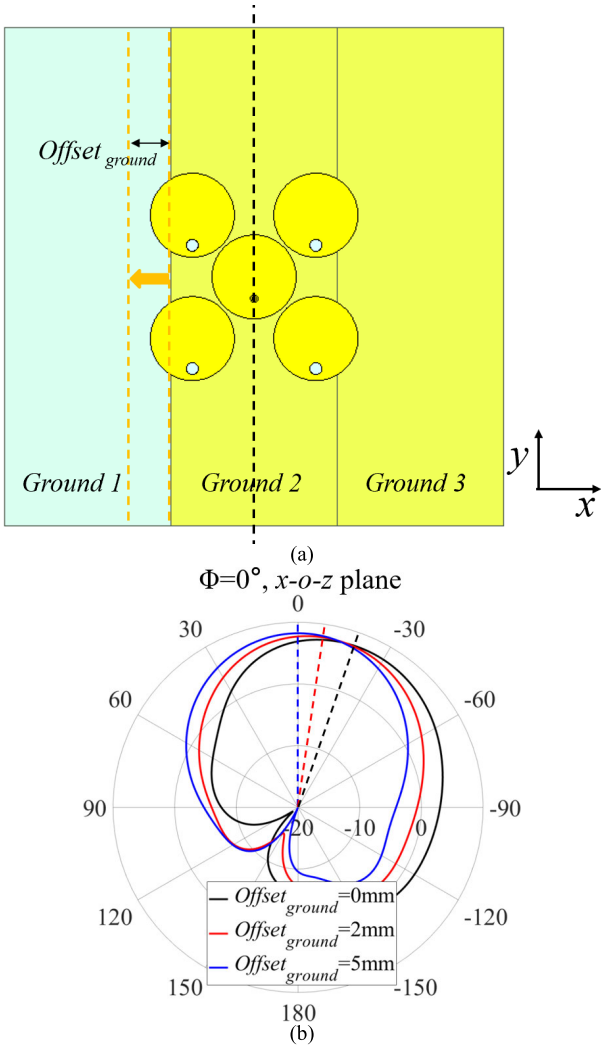

FIGURE 2. Radiation patterns of the proposed antenna when we tune the ground plane made of copper. (a) Geometry of the antenna with copper ground and (b) steerable beams when the copper ground (*Offset*) is tuned.

patch and the parasitics are all circular in shape with the same diameters. Energy is fed into the antenna using a coaxial fed probe. The probe is offset along the y-axis by 4.9 mm in order to yield optimum impedance matching. Each parasitic incorporates a single drill hole which passes through the substrate layer. On the lower surface of the substrate layer, there is a rectangular ground plane named Ground 2. Ground 2 is formed from copper and remains permanently in place. The third layer of the antenna is fabricated from Polylactic acid (PLA) using a 3D printer. It has a thickness of 6 mm, and a permittivity of 2.7. The third layer is located beneath the drill holes. The meandered channels are located in the middle of the third layer. The channel walls, located above and below the channel, are 2 mm thick, as shown in Fig. 1 (c). When the channels are filled with liquid metal, they form Ground 1 and Ground 3. Additionally, the third layer is employed as a cover to prevent the liquid metal from leaking out of the drill holes. A metallic reflector is placed beneath the third layer, as shown in Fig. 1 (c).

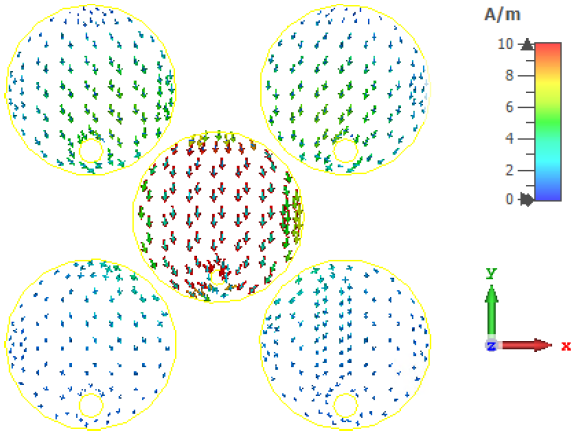

FIGURE 3. The current distribution on the patches of the designed antenna.

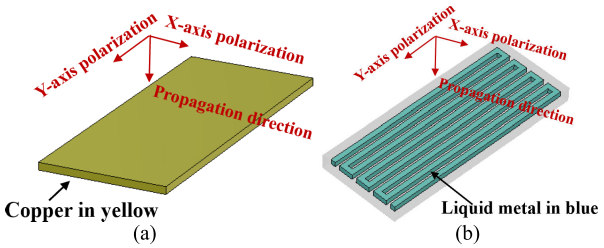

FIGURE 4. Models of (a) a solid metallic ground plane and (b) of the designed meandered channel.

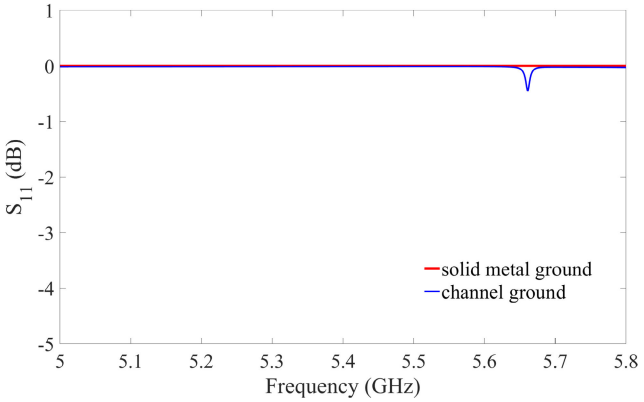

FIGURE 5. The reflection coefficients (S_{11}) of the designed meandered channel and of a solid metallic ground plane shown in Fig. 4 for waves polarized along Y-axis.

B. TUNABLE GROUND TECHNOLOGY

The proposed antenna employs two approaches in unison to steer the direction of the main beam. The first approach involves a tunable ground plane. This is achieved by using liquid metal to form and reshape the ground plane. The segments of ground plane can be continuously tuned, it is only possible

due to the unique properties of liquid metal. Specifically, Ground 1 and Ground 3 are formed from liquid metal. This enables them to be added (On-State) or removed (Off-State) as required. Doing so influences the beam direction. The beam steers towards the direction in which the ground plane has been removed.

TABLE 2. States of tunable grounds and radiation patterns.

	Ground 1	Ground 3	Beam direction
All vias Off	Alter the length of channel by injecting LM from the side near the patches.	On	-10º to 0º
All vias Off	On	Alter the length of channel by injecting LM from the side near the patches.	0º to +10º
Vias A and D On	Alter the length of channel by injecting LM from the side near the patches.	On	-30º to -10º
Vias B and C On	On	Alter the length of channel by injecting LM from the side near the patches.	+10º to +30º

Fig. 2(a) shows a model with simplified tunable ground plane made of copper. The beam steers towards the –X-axis direction when the Ground 3 is On-State. The angle of the main beam can be further controlled by altering the width of Ground 1. This can be achieved by continuously altering the value of $offset_{ground}$. Fig. 2(b) shows the effect of changing $offset_{ground}$ from 0 mm to 5 mm. It can be seen that the beam of the antenna can steer to an angle of 20° with respect to the normal when $offset_{ground}$ is set to 0 mm. The main beam angle decreases when the width of Ground 1 (i.e. $offset_{ground}$) increases. This shows that tuning the ground plane is an effective and novel approach for steering the main beam direction. This approach preserves the symmetry about the Y-axis, thus +X-axis directional beams can be obtained by simply mirroring the states of Grounds.

To achieve the continuous tuning of the ground plane shown in Fig. 2, we designed a meandered channel. Fig. 1 (b) shows the meandered channels for Grounds 1 and 3. The meandered channel designed for use within the proposed antenna has several advantages. Firstly, it enables continuous control of the main beam direction. Secondly, when it is full of liquid metal, it is very similar to a metallic grid along Y-axis, thus blocking waves polarized along the Y-axis. This is significant because the radiation from the patches is directed along the Y-axis. Specifically, Fig. 3 shows the current distribution on the surface of patches. It can be seen that the electric field associated with the driven patch and parasitics is polarized along Y-axis. We have examined and compared the performance of a solid metal ground plane with that of a meandered ground plane. Fig. 4(a) shows a solid metallic ground plane and Fig. 4(b) shows the meandered channel designed for use in the proposed antenna. Both models were excited by waves polarized along the Y-axis and the sides of X-axis and Y-axis were set as periodic boundary conditions. Fig. 5 shows the reflection coefficient (S_{11}) associated with the solid metal ground plane and the proposed meandered channel, shown in Fig. 4. It can be seen that for waves polarized along Y-axis, most of the energy is reflected by the meandered channel and in fact the meandered channel behaves in similar manner to a solid ground plane. For this reason, when the channels are fully filled with liquid metal, we expect them to have the same reflective effect for the main polarization of wave associated with the patches, as a solid metallic ground plane.

Another approach used in the antenna, for beam steering, involves parasitic steering. In the proposed antenna, the central patch acts as the driven element and four surrounding patches act as parasitics. Each parasitic incorporates a single drill hole. The drill holes can be filled or emptied of liquid metal. When all of the drill holes are empty, the parasitics work as directors and the antenna radiates in the boresight direction. When the drill holes are connected to the ground using liquid metal, the associated parasitics work as reflectors and the beam is steered to the opposite direction. The operation principles of this part of the antenna is similar to the principles discussed in the Yagi-Uda which has been described in detail in [25]. However, the design presented in [25] applies parasitic patches which enabled by PIN diodes, whilst the proposed design in this paper combines two different beam steering techniques including: 1) parasitic patches enabled by liquid metal vias and 2) tunable ground plane using liquid metal. This enables the proposed design in this paper to have wider bandwidth performance and more importantly able to continuously steer the beam of the antenna up to ±30° with 1.4 dB of scan loss as will be discussed in the next sections. In addition, the proposed antenna in this paper has the potential for improved and higher power handle capability. However, the design in [25] can only discretely switch beam in few steps to a maximum angle of ±15° with 1.3 dB of scan loss. As a result, the proposed design differs from the design, discussed above, in both approach and performance.

C. BEAM STEERING PERFORMANCE

Due to the meandered channel design, presented in this paper, it is possible to continuously vary the quantity of liquid metal within the channel, and thus achieve continuous beam steering for a patch antenna with a single feed.

Table 2 shows the turning states of the antenna. When all drill holes are empty and the entire ground plane is filled with liquid metal, a broadside beam is obtained. When all of the drill holes are empty and one of the ground plane channels is fully filled with liquid metal, then we can continuously tune the main beam direction by altering the length of the other ground plane channel. Specifically, we continuously inject the liquid metal into meandered channel from the side near the patches, shown in Fig. 6 (a). In this way it is possible to

continuously steer the main beams from ±10° to 0°. When two of the drill holes and one ground plane channel on the same side are simultaneously filled with liquid metal, we can continuously tune the main beam direction by altering the length of the other ground plane channel. Similarly, we continuously inject the liquid metal into meandered channel from the side near the patches, shown in Fig. 6 (b). Under this condition it is possible to continuously steer the main beam direction from ±30° to ±10°.

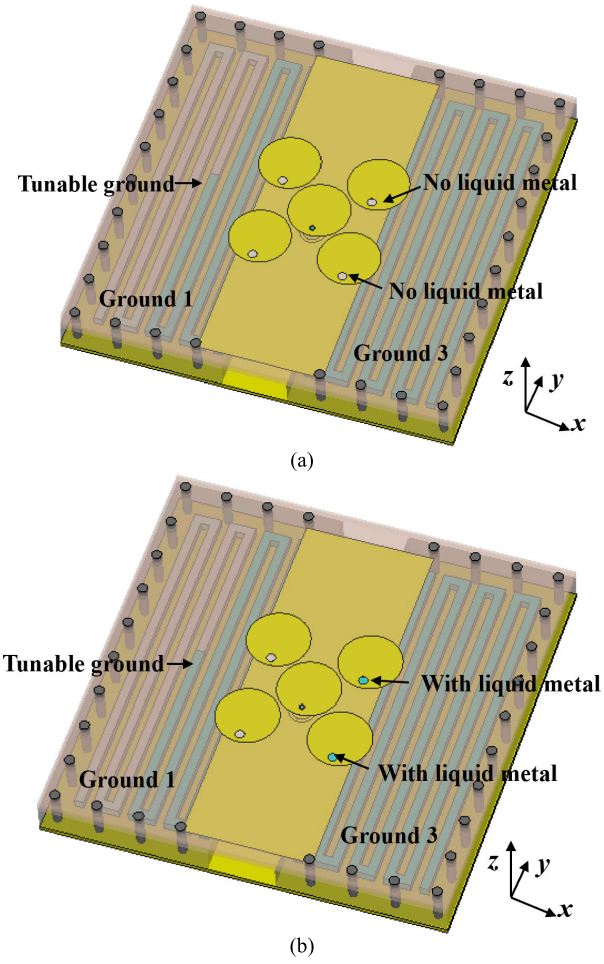

FIGURE 6. Sketch of continuously varying the quantity of liquid metal within the meandered channels. (a) All of the drill holes are empty and the ground plane is continuously tuned, and (b) two of the drill holes are filled with liquid metal and the ground plane is continuously tuned.

All of the simulation results presented in this paper were obtained using CST Microwave Studio 2019. Fig. 7 illustrates the beam steering capability of the antenna in the XZ-plane at 5.3 GHz. Fig. 7(a) shows that the antenna is capable of continuously steering a beam up to a maximum angle of ±30° when we continuously tune the ground plane as shown in Fig. 6. Fig. 7(b) shows a selection of beam directions, namely: 0°, ±10°, ±20°, and ±30°. The simulation result shows that the proposed antenna has a maximum gain of 9 dBi and a scan loss of 1.8 dB across the entire beam scan angle range. Fig. 8 shows the simulated reflection coefficients (S_{11}) associated with the specific main beam directions. It can be seen that the proposed antenna has a −10 dB reflection coefficient bandwidth ranging from 5.3 GHz to 5.5 GHz.

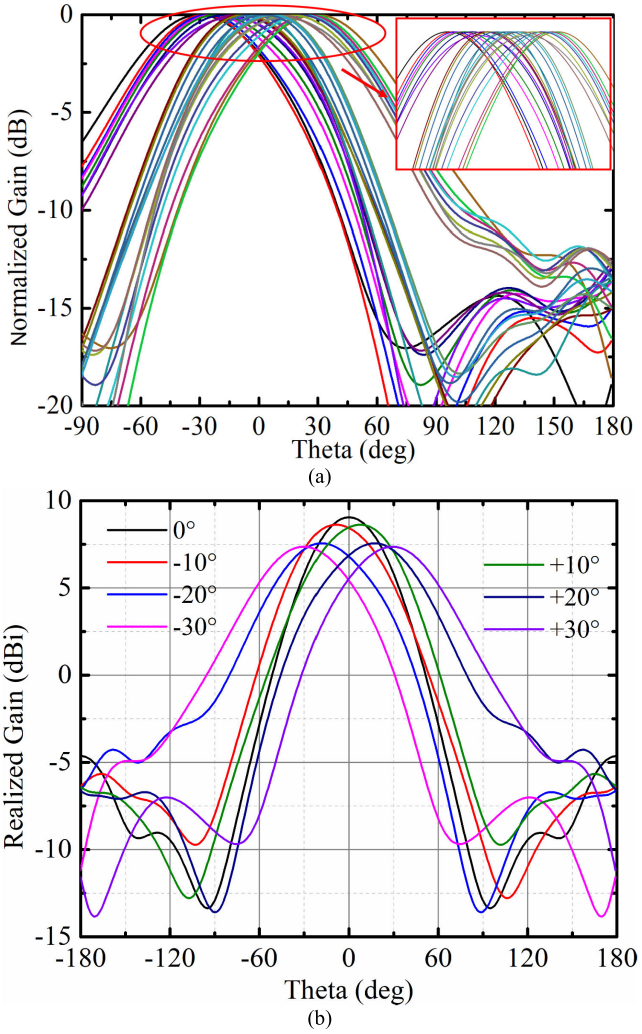

FIGURE 7. Simulated radiation pattern at 5.3 GHz in XZ-plane. (a) Continuous scanning and (b) several beams in XZ-plane.

III. FABRICATION CONSIDERATION AND MEASUREMENT RESULTS

To verify the proposed design, a hardware prototype of the antenna was fabricated and measured. A vector network analyzer (Rohde & Schwarz ZNBT 8) was used for the measurement. The radiation pattern for different operating states were measured in an anechoic chamber using the setup shown in Fig 9. As shown in Fig. 9, antenna under test (AUT) is aligned to a dual polarized transmitter antenna (Tx) and replaced on top of a turning table that rotates 360° in the Azimuth pane. The distance between Tx and AUT is 3.25 m. Both AUT and Tx are connected to Keysight PNA-L N5230C network analyzer to measure AUT radiation patterns. In addition, the gain of the antenna is measured using the gain comparison method described in detail in [26] using the same measurement setup.

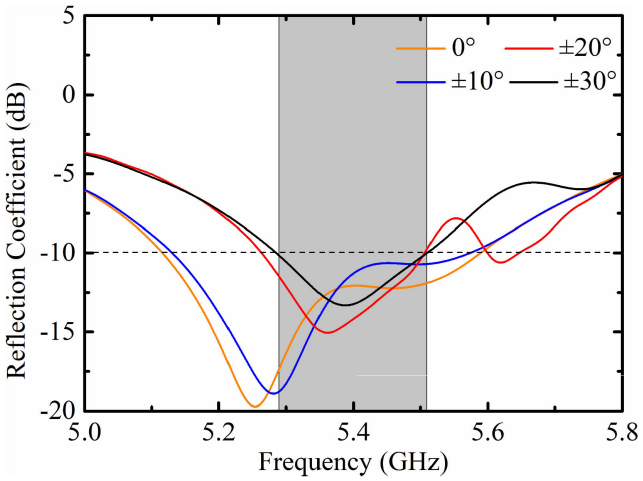

FIGURE 8. The reflection coefficients of the antenna as a function of frequency.

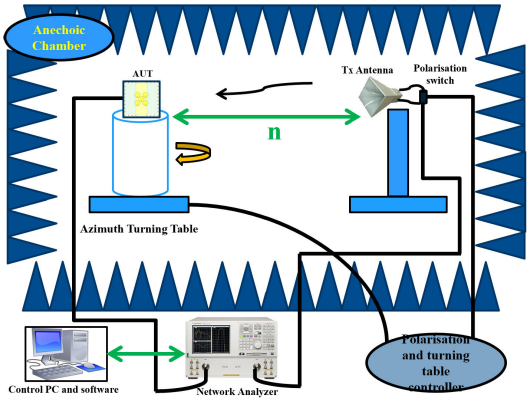

FIGURE 9. The setup used to perform the radiation patterns and gain measurements of the proposed antenna. The distance between Tx antenna and AUT is n = 3.25 m.

A. 3D PRINTING CHANNELS

3D printing technology is employed in the fabrication of meandered channels, which can build virtually any complicated objects. According to the specifications of the 3D printer Ultimaker S3, the finest feature that can be realized in the vertical direction is a 0.06 mm. The material used to print the channel is transparent Polylactic acid (PLA). Nominally PLA has a permittivity of 2.7 and a loss tangent of 0.017 [27]. However, due to the presence of air-filled channels, the effective permittivity of the overall printed objects will be lower than 2.7. This can be explained by the asymmetric Bruggeman (A-BG) effective equation, which calculates the effective permittivity of the printed object.

$$\text{A-BG}: \frac{\varepsilon_i - \varepsilon_{eff}}{\varepsilon_i - \varepsilon_h} = (1-p)\left(\frac{\varepsilon_{eff}}{\varepsilon_h}\right)^{1/3} \quad (1)$$

where: εeff is the effective permittivity of the printed slab, εi is the permittivity of the printing material, εh is the permittivity of the host material, p is the volume fraction of printing material. In our case, the printing material is transparent PLA material with the permittivity of 2.7, and the host material is air with the permittivity of 1.

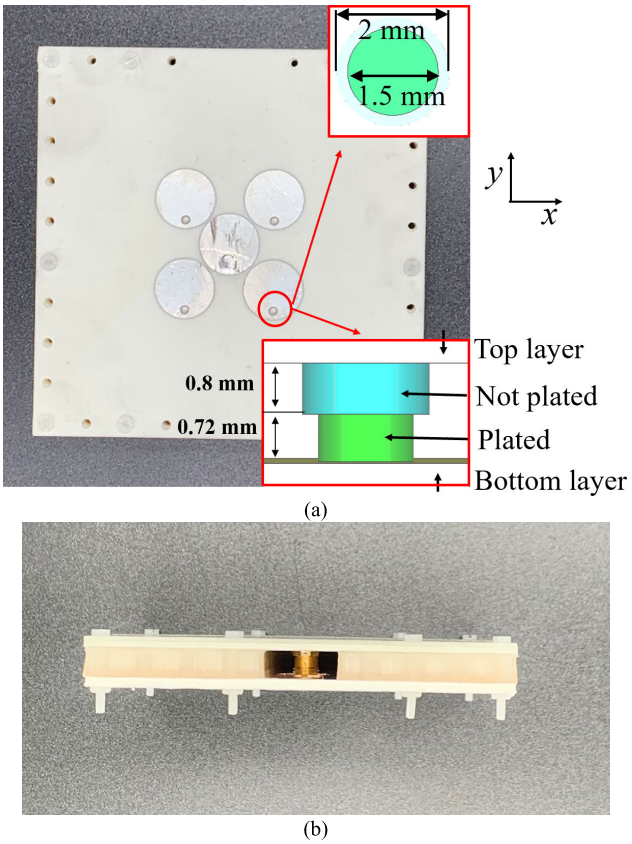

FIGURE 10. The photograph of the fabricated prototype. (a) Top view and (b) side view.

The designed meandered channel enables continuous control of the main beam direction. However, during the measurement, when liquid metal is injected into only part of the channel, i.e. the channel is not fully filled, the position of liquid metal in the channel may alter. The reason for this is that the antenna may be accidentally shaken during the measurement. To solve this problem, we simplify the channel to be some straight ones so that we can measure several typical states where only part of the channel is filled with liquid metal. Such design has the same RF performance as the original design and can fix the liquid metal into the required places.

B. PROTOTYPE OF ANTENNA

Fig. 10 shows a photograph of the fabricated antenna. A series of screws, located around the edge of the substrate, were used to secure the several layers in position. A cover layer is required to prevent the liquid metal from leaking out. The reflector was formed from a piece of substrate incorporating copper on the upper side. The liquid metal employed, for the work reported in this paper, is based around an alloy consisting of 75% Gallium and 25% Indium. The conductivity of this liquid metal is 3.4×10^6 S/m.

The drill holes in the parasitics are used to contain and guide liquid metal. Effectively, therefore the drill holes also form liquid metal channels. It is important to ensure a good electrical connection between the liquid metal in the drill holes and the ground plane. To ensure this, we used a special channel design, see Fig. 10 (a). To ensure that the drill holes were fully filled with liquid metal, we used a multimeter to check the electrical connection between the parasitic patch and the ground plane.

C. INJECTION/REMOVAL OF LIQUIE METAL

The liquid metal was moved into (or withdraw out of) desired positions using a syringe. This technique is widely used in literature within proof-of-concept designs [28], [29], [30], [31], [32]. Fig. 11 (a) shows the actuation of the liquid metal. Fig. 11 (b) shows the different states of tunable ground plane with liquid metal. In this work, altering the method of actuation would have minimal effect on the RF performance of the proposed antenna because the actuation components would be located beneath the metallic reflector, where the electric and magnetic field strengths are minimal. Consequently, for this application, it is possible to control the liquid metal using a micropump [24] or electrochemically controlled capillary action [33]. The electrical technique has been shown capability of moving liquid metal at a rate of 30 cm/s [34]. In our design, the overall length of the meandered channel for one ground (Ground 1 or Ground 3) is 66 cm. In this case, it should be possible to fully fill the ground channel within 2.2 s, and thus the reconfiguration time for our design is expected to range from milliseconds to seconds. Although the switching speed of liquid metal may be slower than conventional electrical devices such as PIN diodes, it still could be used for some applications, such as airport radar and user terminals for satellite internet. Both require switching speeds ranging from milliseconds to seconds but require high power-handling capability and low loss.

D. MEASUREMENT RESULTS

Fig. 12 illustrates the simulation and measurement results associated with a selection of beam directions, namely: 0°, −10°, −20°, and −30° in the XZ-plane. Specifically, when all via holes are empty and Grounds 1 and 3 are On-State, a beam in the boresight direction is obtained. When all via holes are empty and only the Ground 3 is On-State, the beam is steered to −10° direction. When via holes A and D as well as Ground 3 are simultaneously On-State, while Ground 2 is partially filled with liquid metal from the side near the patches, a beam steering of −20° is obtained. When Ground 2 is Off-State, while via holes A and D are On-State as well as Ground 3 is On-State, the beam is steered to −30° direction. It is worth noting that the structure is symmetrical along the Y-axis, and the beams pointing towards +X-axis direction are obtained by simply mirroring the states of vias along with the configuration of the ground plane. The measured results, for all states, agree well with the simulations.

(a)

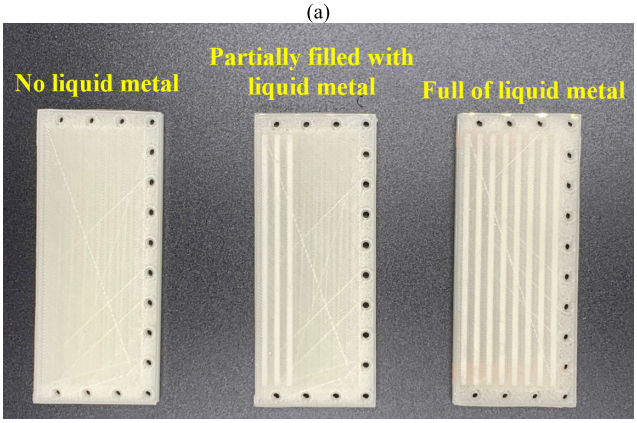

(b)

FIGURE 11. Actuation of the liquid metal. (a) Channels drained by a syringe and (b) channels with liquid metal in different states.

From Fig. 12 (a), (c), (e), and (g), it can be seen that the proposed antenna has an overlapping measured −10 dB reflection coefficient bandwidth ranging from 5.3 GHz to 5.5 GHz. From Fig. 12 (b), (d), (f) and (h), it is clear that the proposed antenna is capable of steering its beams up to a maximum angle of ±30° whilst maintaining a cross-polar radiation below −20 dB. This indicates that the radiation from the antenna is quite strongly linearly polarized. This is expected for a circular microstrip patch antenna. Additionally, the side lobe level (SLL) for all states is lower than 12 dB. The total efficiency of the proposed antenna using liquid metal is more than 85% for all states.

Fig. 13 shows the simulated gains and the measured gains. Fig. 13 (a) shows the gains associated with the different beam angles. It can be seen that, the measured gains for main beam directions towards 0°, ±10°, ±20°, and ±30° are 7.9 dBi, 8.1 dBi, 7 dBi, and 6.7 dBi, respectively. The maximum difference between measured gains and simulated gains is 1 dB. The difference between the simulation and measurement results may be attributable to fabrication errors of PCB as well as 3D printing, assembly errors, and the alignment of the measurement system. Additionally, the simulation results show that the difference in conductivity between liquid metal and copper has little effect on gain degradation for this antenna.

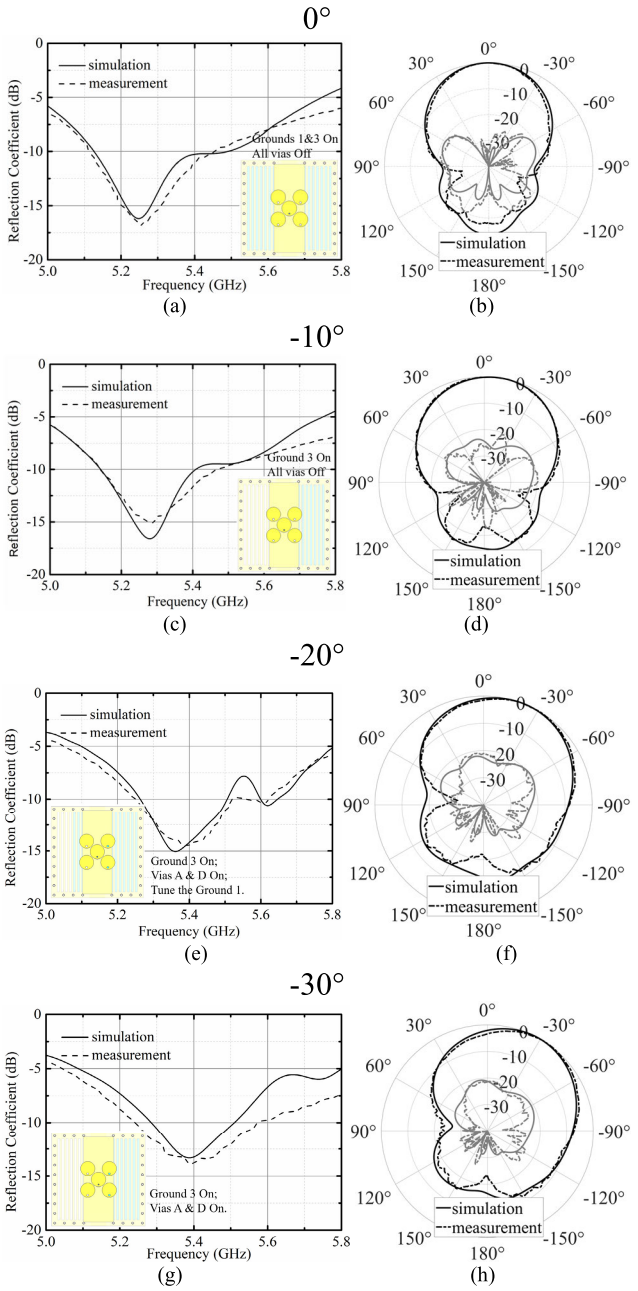

FIGURE 12. Measurement and simulated results associated with four beams directed towards 0°, −10°, −20°, and −30° in the XZ-plane. Figures (a), (c), (e), and (g) show the reflection coefficients (S_{11}) of the antenna, figures (b), (d), (f), and (h) show the radiation patterns.

The measured scan loss is 1.4 dB across the whole beam scan angle range. Fig. 13 (b) shows the gains of broadside beams over a range of different frequencies. The difference between measured gains and simulated gains are all smaller than 1 dB at different frequencies. Table 3 compares the performance of single-element antennas reported previously in the literature against that of the antenna presented in this paper. It can be seen that the proposed antenna has a high performance on relatively wide bandwidth, wide scan angle range, low scan loss and low SLL. Most importantly, compared to designs

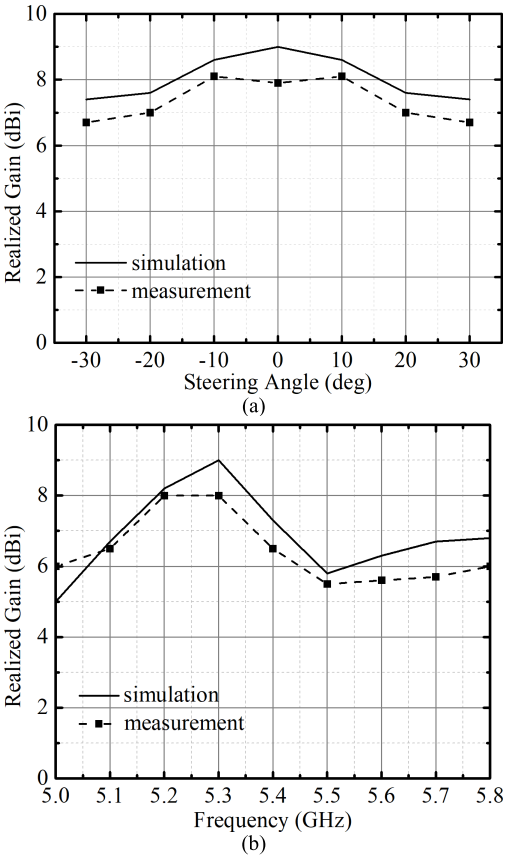

FIGURE 13. Measured and simulated gains (a) versus scanning angles and (b) measured gains and simulated gains of broadside beam versus frequencies.

with PIN diodes and liquid metal in [25], [35], [36], and [37], the proposed antenna has the capability of achieving continuous beam steering. In addition, the proposed antenna has higher overall gain performance than the designs in [24], [35], [36], and [38] and better scanning loss performance than the antennas in [25], [35], [37], and [38]. Finally, the

TABLE 3. Comparison between the Performance of the proposed antenna and other antennas.

Ref.	Freq./ Bandw-idth (GHz/ MHz)	Gain (dBi)	Steer angle	No. of beam	Scan loss (dB)	SLL (dB)	Cont -rol
[25]	2.3/40 (1.7%)	8.2	15°	5	2	15	PIN
[35]	2.45/60 (2.4%)	7.2	±30°	3	1.6	9	PIN
[36]	2.4/150 (6.2%)	6.1	360°	4	0.5	\	PIN
[37]	4.5/500 (11.1%)	8.5	±54°	5	3.1	8	LM
[38]	5/230 (4.6%)	6.3	±43°	continu ous	3	3	Freq.
[24]	1.8/70 (3.8%)	< 3	360°	continu ous	0.5	3	LM
Our work	5.3/200 (3.8%)	8.1	±30°	continu ous	1.4	12	LM

proposed antenna has the potential to handle higher RF power in comparison to other antennas, especially those using PIN diodes as a means of reconfiguration. The latter derives from the fact that the antenna is built using RO4003c substrate, PLA and fed using SMA connector which all have good and high-power handling capabilities. Hence, it is expected that the proposed antenna in this paper to be able to handle high RF power as there would appear to be nothing about liquid metal that should inherently limit its power handling capability.

IV. CONCLUSION

This paper presents a continuously beam-steerable patch antenna using liquid metal. The proposed antenna combines two beam steering methods which are parasitic steering together with a novel tunable ground plane. The tunable ground plane has meandered channels that can be filled with liquid metal. The meander channel was fabricated by 3D printing technology. The unique design of the meandered channel enables continuous control of liquid metal, which makes it possible for antenna to provide continuous beam steering. To the best of our knowledge, this is the first time that tunable ground plane has been used for a patch antenna to achieve continuous beam steering. Such an approach has never been tried before and it is only possible due to the unique properties of liquid metal. The antenna was fabricated and measured. Based on the measurement results, the proposed antenna has a -10 dB reflection coefficient bandwidth ranging from 5.3 GHz to 5.5 GHz with peak measured gain of 8.1 dBi. More importantly, the proposed antenna has the capability of continuously steering its beams to a maximum angle of $\pm 30°$. The measured scan loss and SLL during the entire scan angle range are 1.4 dB and lower than 12 dB, respectively. The proposed antenna is an attractive candidate for modern wireless communications.

ACKNOWLEDGMENT

The authors would like to acknowledge the support from The United Kingdom Engineering and Physical Sciences Research Council [Grant number EP/V008420/1] which funded the production of prototypes and of the Chinese Scholarship Council who funded the first author's Ph.D. studentship. They also acknowledge the support of the QMUL Antenna Lab. For the purpose of open access, the author(s) has applied for a Creative Commons Attribution (CC BY) license to any Accepted Manuscript version arising.

REFERENCES

[1] S. Pan, M. Lin, M. Xu, S. Zhu, L.-A. Bian, and G. Li, "A low-profile programmable beam scanning holographic array antenna without phase shifters," *IEEE Internet Things J.*, vol. 9, no. 11, pp. 8838–8851, Jun. 2022.

[2] Z. Qu, S.-W. Qu, Z. Zhang, S. Yang, and C. H. Chan, "Wide-angle scanning lens fed by small-scale antenna array for 5G in millimeter-wave band," *IEEE Trans. Antennas Propag.*, vol. 68, no. 5, pp. 3635–3643, May 2020.

[3] J. Yun, D. Park, D. Jang, and K. C. Hwang, "Design of an active beam-steering array with a perforated wide-angle impedance matching layer," *IEEE Trans. Antennas Propag.*, vol. 69, no. 9, pp. 6028–6033, Sep. 2021.

[4] A. K. Singh, M. P. Abegaonkar, and S. K. Koul, "Wide angle beam steerable high gain flat top beam antenna using graded index metasurface lens," *IEEE Trans. Antennas Propag.*, vol. 67, no. 10, pp. 6334–6343, Oct. 2019.

[5] P. Mei, S. Zhang, and G. F. Pedersen, "A low-cost, high-efficiency and full-metal reflectarray antenna with mechanically 2-D beam-steerable capabilities for 5G applications," *IEEE Trans. Antennas Propag.*, vol. 68, no. 10, pp. 6997–7006, Oct. 2020.

[6] R. Rodriguez-Cano, S. Zhang, K. Zhao, and G. F. Pedersen, "Mm-wave beam-steerable endfire array embedded in a slotted metal-frame LTE antenna," *IEEE Trans. Antennas Propag.*, vol. 68, no. 5, pp. 3685–3694, May 2020.

[7] E. Abdo-Sánchez, D. Palacios-Campos, C. Frías-Heras, F. Y. Ng-Molina, and T. M. Martín-Guerrero, "Electronically steerable and fixed-beam frequency-tunable planar traveling-wave antenna," *IEEE Trans. Antennas Propag.*, vol. 64, no. 4, pp. 1298–1306, Apr. 2016.

[8] R. O. Ouedraogo, E. J. Rothwell, and B. J. Greetis, "A reconfigurable microstrip leaky-wave antenna with a broadly steerable beam," *IEEE Trans. Antennas Propag.*, vol. 59, no. 8, pp. 3080–3083, Aug. 2011.

[9] J. Hu, Y. Li, and Z. Zhang, "A novel reconfigurable miniaturized phase shifter for 2-D beam steering 2-bit array applications," *IEEE Microw. Wireless Compon. Lett.*, vol. 31, no. 4, pp. 381–384, Apr. 2021.

[10] Z. Wang, F. Zhang, H. Gao, O. Franek, G. F. Pedersen, and W. Fan, "Over-the-air array calibration of mmWave phased array in beam-steering mode based on measured complex signals," *IEEE Trans. Antennas Propag.*, vol. 69, no. 11, pp. 7876–7888, Nov. 2021.

[11] B. Schaer, K. Rambabu, J. Bornemann, and R. Vahldieck, "Design of reactive parasitic elements in electronic beam steering arrays," *IEEE Trans. Antennas Propag.*, vol. 53, no. 6, pp. 1998–2003, Jun. 2005.

[12] Y. Xiong, X. Zeng, and J. Li, "A tunable concurrent dual-band phase shifter MMIC for beam steering applications," *IEEE Trans. Circuits Syst. II, Exp. Briefs*, vol. 67, no. 11, pp. 2412–2416, Nov. 2020.

[13] P. Qin, L. Song, and Y. J. Guo, "Beam steering conformal transmitarray employing ultra-thin triple-layer slot elements," *IEEE Trans. Antennas Propag.*, vol. 67, no. 8, pp. 5390–5398, Aug. 2019.

[14] B. Rana, I.-G. Lee, and I.-P. Hong, "Digitally reconfigurable transmitarray with beam-steering and polarization switching capabilities," *IEEE Access*, vol. 9, pp. 144140–144148, 2021.

[15] G.-B. Wu, S.-W. Qu, S. Yang, and C. H. Chan, "Low-cost 1-D beam-steering reflectarray with $\pm 70°$ scan coverage," *IEEE Trans. Antennas Propag.*, vol. 68, no. 6, pp. 5009–5014, Jun. 2020.

[16] O. Kiris, K. Topalli, and M. Unlu, "A reflectarray antenna using hexagonal lattice with enhanced beam steering capability," *IEEE Access*, vol. 7, pp. 45526–45532, 2019.

[17] I. J. Nam, S. M. Lee, and D. H. Kim, "Miniaturized beam reconfigurable reflectarray antenna with wide 3-D beam coverage," *IEEE Trans. Antennas Propag.*, vol. 70, no. 4, pp. 2613–2622, Apr. 2022.

[18] W. Cao, Y. Xiang, B. Zhang, A. Liu, T. Yu, and D. Guo, "A low-cost compact patch antenna with beam steering based on CSRR-loaded ground," *IEEE Antennas Wireless Propag. Lett.*, vol. 10, pp. 1520–1523, 2011.

[19] S.-J. Ha and C. W. Jung, "Reconfigurable beam steering using a microstrip patch antenna with a U-slot for wearable fabric applications," *IEEE Antennas Wireless Propag. Lett.*, vol. 10, pp. 1228–1231, 2011.

[20] G. Yang, J. Li, D. Wei, S.-G. Zhou, and R. Xu, "Pattern reconfigurable microstrip antenna with multidirectional beam for wireless communication," *IEEE Trans. Antennas Propag.*, vol. 67, no. 3, pp. 1910–1915, Mar. 2019.

[21] J. Ouyang, Y. M. Pan, and S. Y. Zheng, "Center-fed unilateral and pattern reconfigurable planar antennas with slotted ground plane," *IEEE Trans. Antennas Propag.*, vol. 66, no. 10, pp. 5139–5149, Oct. 2018.

[22] H. A. Majid, M. K. A. Rahim, M. R. Hamid, and M. F. Ismail, "Frequency and pattern reconfigurable slot antenna," *IEEE Trans. Antennas Propag.*, vol. 62, no. 10, pp. 5339–5343, Oct. 2014.

[23] T. Aboufoul, C. Parini, X. C. Chen, and A. Alomainy, "Pattern-reconfigurable planar circular ultra-wideband monopole antenna," *IEEE Trans. Antennas Propag.*, vol. 61, no. 10, pp. 4973–4980, Oct. 2013.

[24] D. Rodrigo, L. Jofre, and B. A. Cetiner, "Circular beam-steering reconfigurable antenna with liquid metal parasitics," *IEEE Trans. Antennas Propag.*, vol. 60, no. 4, pp. 1796–1802, Apr. 2012.

[25] M. Jusoh, T. Sabapathy, M. F. Jamlos, and M. R. Kamarudin, "Reconfigurable four-parasitic-elements patch antenna for high-gain beam switching application," *IEEE Antennas Wireless Propag. Lett.*, vol. 13, pp. 79–82, 2014.

[26] C. A. Balanis, "Antenna measurement," in *Antenna Theory*, vol. 2, 3rd ed. Hoboken, NJ, USA: Wiley, 2005, ch. 17, sec. 4, pp. 1033–1034.
[27] J. Zechmeister and J. Lacik, "Complex relative permittivity measurement of selected 3D-printed materials up to 10 GHz," in *Proc. Conf. Microw. Techn. (COMITE)*, Apr. 2019, pp. 1–4.
[28] W. Chen, Y. Li, R. Li, A. V.-Y. Thean, and Y.-X. Guo, "Bendable and stretchable microfluidic liquid metal-based filter," *IEEE Microw. Wireless Compon. Lett.*, vol. 28, no. 3, pp. 203–205, Mar. 2018.
[29] C. Koo, B. E. LeBlanc, M. Kelley, H. E. Fitzgerald, G. H. Huff, and A. Han, "Manipulating liquid metal droplets in microfluidic channels with minimized skin residues toward tunable RF applications," *J. Microelectromech. Syst.*, vol. 24, no. 4, pp. 1069–1076, Aug. 2015.
[30] M. A. Rafi, B. D. Wiltshire, and M. H. Zarifi, "Wideband tunable modified split ring resonator structure using liquid metal and 3-D printing," *IEEE Microw. Wireless Compon. Lett.*, vol. 30, no. 5, pp. 469–472, May 2020.
[31] A. M. Watson, T. F. Leary, K. S. Elassy, A. G. Mattamana, M. A. Rahman, W. A. Shiroma, A. T. Ohta, and C. E. Tabor, "Physically reconfigurable RF liquid electronics via Laplace barriers," *IEEE Trans. Microw. Theory Techn.*, vol. 67, no. 12, pp. 4881–4889, Dec. 2019.
[32] L. Song, W. Gao, C. O. Chui, and Y. Rahmat-Samii, "Wideband frequency reconfigurable patch antenna with switchable slots based on liquid metal and 3-D printed microfluidics," *IEEE Trans. Antennas Propag.*, vol. 67, no. 5, pp. 2886–2895, May 2019.
[33] M. Wang, M. R. Khan, C. Trlica, M. D. Dickey, and J. J. Adams, "Pump-free feedback control of a frequency reconfigurable liquid metal monopole," in *Proc. IEEE Int. Symp. Antennas Propag. USNC/URSI Nat. Radio Sci. Meeting*, Jul. 2015, pp. 2223–2224.
[34] M. R. Khan, C. Trlica, and M. D. Dickey, "Recapillarity: Electrochemically controlled capillary withdrawal of a liquid metal alloy from microchannels," *Adv. Funct. Mater.*, vol. 25, no. 5, pp. 671–678, Feb. 2015.
[35] Z.-L. Lu, X.-X. Yang, and G.-N. Tan, "A multidirectional pattern-reconfigurable patch antenna with CSRR on the ground," *IEEE Antennas Wireless Propag. Lett.*, vol. 16, pp. 416–419, 2017.
[36] F. Farzami, S. Khaledian, B. Smida, and D. Erricolo, "Pattern-reconfigurable printed dipole antenna using loaded parasitic elements," *IEEE Antennas Wireless Propag. Lett.*, vol. 16, pp. 1151–1154, 2017.
[37] V. T. Bharambe and J. J. Adams, "Planar 2-D beam steering antenna using liquid metal parasitics," *IEEE Trans. Antennas Propag.*, vol. 68, no. 11, pp. 7320–7327, Nov. 2020.
[38] H. Tian, K. Dhwaj, L. J. Jiang, and T. Itoh, "Beam scanning realized by coupled modes in a single-patch antenna," *IEEE Antennas Wireless Propag. Lett.*, vol. 17, no. 6, pp. 1077–1080, Jun. 2018.

ZHISHU QU was born in China, in 1993. She received the B.S. and M.S. degrees in electromagnetic field and microwave technology from the University of Electronic Science and Technology of China (UESTC), Chengdu, China, in 2016 and 2019, respectively. She is currently pursuing the Ph.D. degree with the Queen Mary University of London (QMUL), London, U.K.

Her research interests include dielectric lens, phased arrays, millimeter-wave antennas, 3-D printed antennas, and reconfigurable liquid metal antennas.

YIHUA ZHOU (Graduate Student Member, IEEE) was born in China, in 1993. She received the B.Sc. and M.Sc. degrees from the Nanjing University of Science and Technology (NUST), Nanjing, China, in 2016 and 2019, respectively. She is currently pursuing the Ph.D. degree with the School of Electronic Engineering and Computer Science, Queen Mary University of London, London, U.K.

Her current research interests include microwave reconfigurable liquid metal antennas and 3-D printed antennas.

SHAKER ALKARAKI (Member, IEEE) received the B.Sc. degree (Hons.) in communication engineering from IIUM Malaysia, Selangor, Malaysia, in 2011, the M.Sc. degree (Hons.) from The University of Manchester (UoM), Manchester, U.K., in 2013, and the Ph.D. degree in electronic engineering from the Queen Mary University of London (QMUL), London, U.K., in 2019. He is currently a Postdoctoral Researcher with the Antennas and Electromagnetics Group, QMUL. He is the holder of IIUM B.Sc. Scholarship, UoM M.Sc. Scholarship, and QMUL Ph.D. Scholarship. His research interests include millimeter-wave (mm-wave) and microwave reconfigurable devices, mm-wave antennas and arrays, 3-D printed antennas, metallization techniques, 5G antennas and systems, multi-in multi-out (MIMO), leaky waves, and reconfigurable liquid metal (LM) antennas.

JAMES R. KELLY (Member, IEEE) received the master's degree in electronic and electrical engineering and the Ph.D. degree in microwave filters from Loughborough University, Loughborough, U.K., in 2002 and 2007, respectively. From 2007 to 2012, he worked as a Postdoctoral Researcher with Loughborough University; University of Birmingham, Birmingham, U.K.; University of Durham, Durham, U.K.; and The University of Sheffield, Sheffield, U.K. From 2012 to 2013, he was a Lecturer with Anglia Ruskin University, Cambridge, U.K. In 2013, he joined the Institute for Communication Systems (ICS), University of Surrey, Guildford, U.K. In 2018, he joined the Queen Mary University of London, London, U.K., where he is employed as a Lecturer of microwave antennas. He has authored over 100 academic articles in peer-reviewed journals and conference proceedings. He holds a European patent on reconfigurable antennas. His research interest includes reconfigurable antennas. He is a member of the Institution of Engineering and Technology (IET).

YUE GAO (Senior Member, IEEE) received the Ph.D. degree from the Queen Mary University of London (QMUL), U.K., in 2007. He is currently a Professor at the School of Computer Science and the Director of the Intelligent Networking and Computing Research Centre, Fudan University, China. He worked as a Lecturer, a Senior Lecturer, a Reader, and the Chair Professor at QMUL and the University of Surrey, respectively. His research interests include smart antennas, sparse signal processing, and cognitive networks for mobile and satellite systems. He has published over 200 peer-reviewed journal and conference papers and had over 6400 citations. He is a member of the Board of Governors. He was also elected as an Engineering and Physical Sciences Research Council fellow in 2017. He was a co-recipient of the EU Horizon Prize Award on collaborative spectrum sharing in 2016. He is a Distinguished Speaker of the IEEE Vehicular Technology Society (VTS). He is the Vice-Chair of the IEEE ComSoc Wireless Communication Technical Committee and the past Chair of the IEEE ComSoc Technical Committee on Cognitive Networks. He has been the Symposia Chair, the Track Chair, and other roles in the organising committee of several IEEE ComSoC, VTS, and other conferences. He has been an Editor of several IEEE TRANSACTIONS and journals.